

DYNAMIC RESPONSE OF OBJECTS WITH SHOCK-ABSORBERS TO SEISMIC LOADS

E. Ya. Antonyuk and V. V. Timokhin

UDC 531.38

The paper outlines a mathematical model describing the vibrations of buildings and engineering structures with general-type passive shock-absorbers, rigid bodies, and ideal constraints. Two modifications of systems with passive shock absorbers are considered assuming constancy of their structure. These systems are studied numerically; the dynamic processes excited in them are compared

Keywords: seismic acceleration, contact surfaces, ideal constraint, rigid body, excitation, dynamic processes

Introduction. Considerable damage and numerous victims of earthquakes challenge researchers to look for ways of minimizing the effect of such phenomena. The design of buildings is improved to enhance their capability of resisting loads due to vibrations of the foundation (ground). Dynamic loads on various mechanical systems can significantly be reduced by using shock-absorbing devices with flexible, frictional, and other elements [7, 13–15]. Currently, various shock-absorbers are intensively used to reduce seismic loads on buildings and above-ground structures [2, 9, 11, 16, 17]. Relevant research efforts are important because of the destructive earthquake in Japan (Kobe, 1995) and, for example, the recent (2005–2006) earthquakes in Indonesia, Thailand, China, Turkey, Iran, Russia (Koryakiya), Pakistan, and other regions of the globe. This problem is also of importance for Ukraine, especially for the Crimea, the Carpathians, and adjacent regions. There has been a recent resurgence of interest in new designs and structures of seismic dampers with high damping capabilities owing to rubber and plastic elements and coatings [11]. Despite the different designs of the passive shock-absorbers to be discussed below, their mathematical models in a general dynamic system have a stereotypic description for many modifications.

This paper outlines a deterministic model of a system with general-type passive seismic dampers and compares two modifications of this kind of shock-absorbers to assess how they reduce the inertial effect of an earthquake on a shock-mounted body (building or engineering structure). All components of the system are considered rigid. The translational motion exciting the system is considered kinematic and is specified as time-dependent accelerations. It is adopted that the maximum accelerations range from 0.2 to 0.4 m/sec², the duration of excitation from 10 to 40 sec, and the dominant periods in the excitation spectrum from 0.1 to 2 sec [4, 6]. The constraints are assumed ideal, i.e., the work done by constraint forces against a possible displacement is zero. Moreover, the constraints among bodies are considered to be ideal, holonomic, and bilateral. As possible examples, we will use the systems shown in Fig. 1 [2, 8, 9, 17], where component 1 is the body (foundation) undergoing oscillatory motions with seismic acceleration $W_x = \ddot{x}_1$, and component 2 is the body (engineering structure) subject to the dynamic load from the foundation. The contacting surfaces of bodies 1 and 2 (Fig. 1a) or bodies 2 and 3 (Fig. 1b) are represented by circular arcs of radii R and r (in the plane of the figure); other curves can also be used for this purpose. Since the coefficient of friction of the second kind (rolling friction) has small values (according to [11], it ranges from 0.03 to 0.06 in shock-absorbers with a viscous layer on its contact surfaces), this type of friction is neglected in the mathematical model. Also, sliding friction is considered absent in the system in Fig. 1b, i.e., the contact surfaces of bodies 1 and 2 are assumed perfectly smooth. The sliding friction in the system in Fig. 1b is assumed sufficient to ensure rolling without slipping, i.e., the contact surfaces of bodies 1 and 3 and bodies 2 and 3 are absolutely rough [3].

Rolling bodies 3 (Fig. 1b) are assumed inertialess. The model is based on the Lagrange equations of the first kind. It will be used to numerically analyze the processes in a dynamic system with shock-absorbers of two types subject to seismic accelerations and to compare the effectiveness of these shock-absorbers.

S. P. Timoshenko Institute of Mechanics, National Academy of Sciences of Ukraine, Kyiv. Translated from *Prikladnaya Mekhanika*, Vol. 43, No. 12, pp. 127–137, December 2007. Original article submitted November 3, 2006.

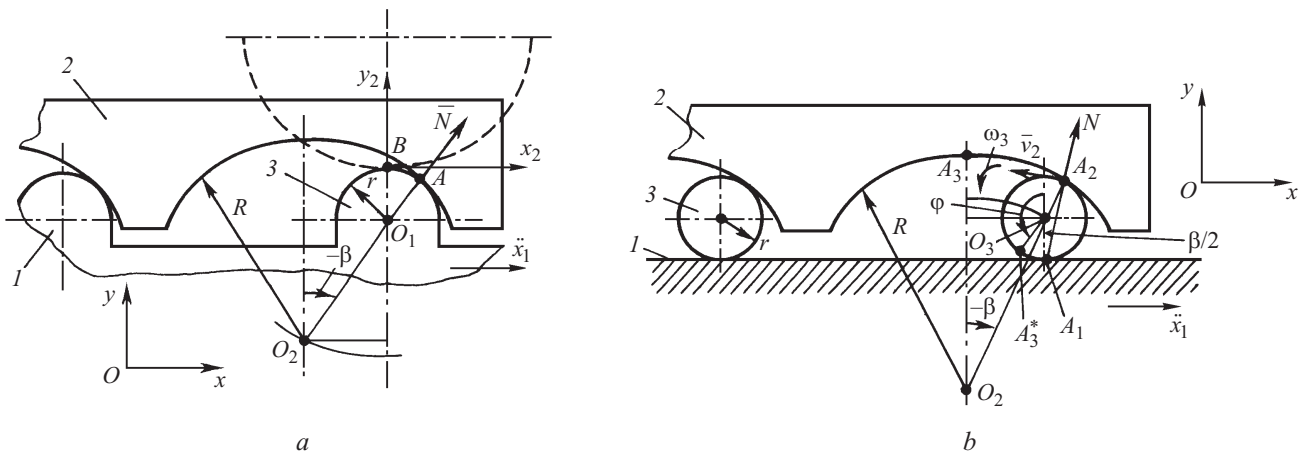


Fig. 1

1. Kinematic Relations. The features of the system in question suggest that it is most convenient to use the Lagrange equations of the first kind for the model. In that case, the equations of motion of the shock-mounted body include constraint equations determined by the design model and contacting surfaces. Naturally, the shock-mounted body rests on several identical supports (ideally, there are three supports and they form a triangle when viewed from above; with more than three supports, measures should be taken to make the system statically determinate [1, 5]).

We will address the constraint equation of the system in Fig. 1a. Let the origin of the coordinate system x_2y_2 be at the point B (the upper end of the vertical diameter of jut 3 of body 1). The coordinates x_2 and y_2 describe the displacements of body 2 relative to body 1. Here is the parametric form of these coordinates:

$$x_2 = (R-r)\sin\beta, \quad (1.1)$$

$$y_2 = (R-r) - (R-r)\cos\beta = (R-r)(1-\cos\beta), \quad (1.2)$$

where the angle β is measured counter-clockwise.

Eliminating the parameter β from (1.1) and (1.2), we obtain the equation of circle

$$x_2^2 + [y_2 - (R-r)]^2 = (R-r)^2. \quad (1.3)$$

Since the relative positions of bodies 1 and 2 are physically realizable, the constraint equation derived from (1.3) describes a semicircle of radius $(R-r)$ below the horizontal diameter (the dashed line in Fig. 1a):

$$y_2 = -\sqrt{(R-r)^2 - x_2^2} + R-r, \quad 0 \leq y_2 \leq R-r. \quad (1.4)$$

The motion of body 2 in the system in Fig. 1b will also be translational because of a similar arrangement of identical supports. The angle β is also assumed positive when measured counter-clockwise. The displacements of body 2 relative to body 1 are defined by the coordinates x_2 and y_2 . The equation of geometrical constraint (between bodies 1 and 2) is convenient to set up in kinematic form, provided that there is no slipping between body 3 and bodies 1 and 2 due to the ideality of the constraints.

The projection of the velocity of the center O_3 of body 3 translating relative to body 1 onto the Ox -axis is given by

$$\dot{x}_{O_3} = -\omega_3 r, \quad (1.5)$$

where ω_3 is the angular velocity of rotation of body 3 in the plane yOx ; r is its radius.

The projection of the relative velocity \bar{v}_2 of body 2 (of any of its points, including A_2) onto the Ox -axis can be found from the condition that the point A_1 is the instantaneous center of relative velocities of body 2, the velocity vector \bar{v}_2 being perpendicular to the position vector A_1A_2 . Thus, we have

$$\dot{x}_2 = -2\omega_3 r \cos\frac{\beta}{2} \cos\frac{\beta}{2}, \quad (1.6)$$

i.e., the absolute angular velocity of rotation of body 3 is

$$\omega_3 = -\frac{\dot{x}_2}{r(1+\cos\beta)}. \quad (1.7)$$

On the other hand, the relative velocity v_{O_3} of the center O_3 of body 3 can be expressed in terms of the velocity \dot{x}_2 of the center O_2 of translating body 2 and the velocity $-\dot{\beta}(R-r)$ of relative revolution of the point O_3 around the pole O_2 (compound motion), which when projected onto the Ox -axis yields

$$\dot{x}_{O_3} = \dot{x}_2 - \dot{\beta}(R-r)\cos\beta, \quad (1.8)$$

where R is the radius of the contact surface of body 2.

As a result, Eqs. (1.5)–(1.8) yield the constraint equation for the coordinates β and x_2 in kinematic form:

$$\dot{\beta} = \frac{\dot{x}_2}{(R-r)(1+\cos\beta)}. \quad (1.9)$$

This equation can be integrated. Using $\beta(u)_0 = 0$ as an initial condition (sphere 3 is located symmetrically about the spherical surface of body 2), we obtain the constraint equation

$$x_2 = (R-r)(\beta + \sin\beta), \quad (1.10)$$

i.e., the constraint is holonomic.

Naturally, the constraint equation (1.10) can also be obtained by considering the conditions of rolling without slipping of cylinder 3 over bodies 1 and 2. After the system moves from the starting position ($\beta = 0$) into the position shown in Fig. 1b, the coordinate x_2 of body 2 is determined from

$$x_2 = x_{O_3} + (R-r)\sin\beta, \quad (1.11)$$

where x_{O_3} is the coordinate of the center O_3 relative to the center O_2 of body 2, φ is the absolute angle of rotation of body 3 rolling over the cylinder of radius R from the point A_3 ($\beta = 0$) to the point A_2 . Since there is no slipping during rolling, the arcs

$$\cup A_2 A_3^* = -r(\varphi - \beta) \quad (1.12)$$

and

$$\cup A_2 A_3 = -\beta R \quad (1.13)$$

are equal, where A_3^* is a point on cylinder 3 initially ($\beta = 0$) coinciding with the A_3 on body 2. Equalities (1.12) and (1.13) yield

$$\varphi = -\beta \left(\frac{R-r}{r} \right). \quad (1.14)$$

The relative coordinate x_{O_3} of the center of body 3 is determined, according to Fig. 1b, as

$$x_{O_3} = -\varphi r. \quad (1.15)$$

In view of (1.14) and (1.15), Eq. (1.11) takes the form (1.10) obtained earlier.

According to Fig. 1b, the constraint equation for the coordinates β and y_2 (for body 2) is

$$y_2 = (R-r)(1-\cos\beta), \quad (1.16)$$

y_2 being reckoned from the upper end of the vertical diameter of cylinder 3.

2. Equations of Motion. In setting up the equations of motion of the systems in Figs. 1a and 1b, it should be born in mind that body 2 undergoes plane translation, i.e., its kinematics is completely characterized by the motion of one point. Of three degrees of freedom (for the plane motion of a free body), rigid body 2 maintains one degree of freedom due to the two constraints

at the contact with two supports. Thus, one equation of motion is enough. It is possible to use the constraint equation $y = f(x)$ between the coordinates x and y of a representative point of body 2 and the associated relationship $\dot{y} = f'(x)\dot{x}$ between the projections of the velocity of the point onto the coordinates axes to derive an equation of motion based on the Lagrange equations of the second kind. This, however, would involve labor-intensive (in some cases) transformations, and, moreover, the ideal constraints among the bodies would not be directly defined. Therefore, it appears more expedient to follow another way: use the Lagrange equations of the first kind and constraint equations and perform matrix transformations employing relevant software such as MATLAB.

In doing so, we obtain, for the systems in Fig. 1, a differential equation of motion and a formula for the undetermined Lagrange multiplier that leads directly to the constrain reaction. We will follow this approach here to develop a model.

The acceleration of the compound motion of an arbitrary point C relative to the inertial frame of reference xOy undergoing plane translation is defined by

$$\ddot{\bar{Z}}_C = \ddot{\bar{Z}} + \bar{W}, \quad (2.1)$$

where \bar{Z} is the position vector of the point C in the coordinate system x_2By_2 ; \bar{Z}_C is the position vector of a point in the absolute frame xOy ; and \bar{W} is the seismic acceleration of body 1 in the same frame of reference. The equation of motion of a point in the frame xOy can be written as

$$m\ddot{\bar{Z}}_C = \bar{P} + \bar{N}, \quad (2.2)$$

where $\bar{P} = m\bar{g}$ is the weight of body 2; \bar{N} is the resultant of the forces exerted by the juts of body 1 or by bodies 3 on body 2 (this resultant is directed along the normals to the surfaces of bodies 1 and 2 at the contact points for the system in Fig. 1a and at the angle $\beta/2$ for the system in Fig. 1b; \bar{g} is the acceleration of gravity; m is the mass of body 2). Substituting (2.1) into (2.2) and performing transformations, we obtain

$$\ddot{\bar{Z}} = \bar{g} + \frac{\bar{N}}{m} - \bar{W}. \quad (2.3)$$

Let us write Eq. (2.3) in matrix form. The elements of the matrix are the projections of the vectors onto the axes of xOy :

$$\begin{bmatrix} \ddot{x}_2 \\ \ddot{y}_2 \end{bmatrix} = \begin{bmatrix} 0 \\ -g \end{bmatrix} + \frac{1}{m} \begin{bmatrix} N_x \\ N_y \end{bmatrix} - \begin{bmatrix} W_x \\ W_y \end{bmatrix}, \quad (2.4)$$

where $Z = \begin{bmatrix} x_2 \\ y_2 \end{bmatrix}$; x_2 and y_2 are the coordinates of the point C in the frame x_2By_2 .

The constraint equation has the parametric ($q = \beta$, Fig. 1) form (1.1), (1.2) for the system in Fig. 1a, i.e., $x_2 = f_1(q)$ and $y_2 = f_2(q)$, and the form (1.10), (1.16) for the system in Fig. 1b. Then $\dot{Z} = \begin{bmatrix} f_1' \\ f_2' \end{bmatrix} \cdot \dot{q}$, where f_1' and f_2' are the derivatives of the

constraint equations with respect to the parameter q . Denoting $C = \begin{bmatrix} f_1' \\ f_2' \end{bmatrix}$, we obtain

$$\dot{Z} = C\dot{q}, \quad (2.5)$$

$$\ddot{Z} = \dot{C}\dot{q} + C\ddot{q}. \quad (2.6)$$

Let $G = \begin{bmatrix} -f_2' \\ f_1' \end{bmatrix}$. Then $G^T C = C^T G = 0$, i.e., the vectors C and G are perpendicular.

Since the vectors C and \dot{Z} are parallel, the vectors G and N are parallel too; therefore, we can write the following expression [10]:

$$N = \lambda G, \quad (2.7)$$

where λ is a scalar (Lagrangian multiplier). Then (2.3) becomes

$$C\ddot{q} + \dot{C}\dot{q} = S + \frac{\lambda G}{m}, \quad (2.8)$$

where $S = \begin{bmatrix} -W_x \\ -g - W_y \end{bmatrix}$ and $\dot{C} = \begin{bmatrix} f_1'' \\ f_2'' \end{bmatrix} \dot{q}$.

Multiply (2.8) by the vector C^T :

$$C^T C\ddot{q} + C^T \dot{C}\dot{q} = C^T S. \quad (2.9)$$

Multiply (2.8) by the vector G^T :

$$G^T \dot{C}\dot{q} = \frac{\lambda G^T G}{m} + G^T S. \quad (2.10)$$

The acceleration \ddot{q} can be found from (2.9), and the multiplier λ from (2.10):

$$\ddot{q} = \frac{-f_1' W_x - f_2' (g + W_y) - (f_1' f_1'' + f_2' f_2'') \dot{q}^2}{(f_1')^2 + (f_2')^2}, \quad (2.11)$$

$$\lambda = \left(\frac{G^T \dot{C}\dot{q} - G^T S}{G^T G} \right) m. \quad (2.12)$$

Expand expression (2.12):

$$\lambda = \left[\frac{(-f_1'' f_2' + f_1' f_2'') \dot{q}^2 - f_2' W_x + f_1' (g + W_y)}{(f_1')^2 + (f_2')^2} \right] m. \quad (2.13)$$

For the system in Fig. 1a, we have

$$x_2 = f_1(q) = \rho \sin q, \quad y_2 = f_2(q) = \rho(1 - \cos q), \quad q = \beta, \quad (2.14)$$

where $\rho = R - r$, R and r are the radii of the contact surfaces of upper (2) and lower (1) bodies in Fig. 1a, respectively.

Substituting (2.14) into (2.11) and (2.13), we obtain an equation of motion of body 2 and an equation to determine the variable coefficient λ and, hence, the reaction N :

$$\begin{aligned} \ddot{q} &= -\frac{1}{\rho} (W_x \cos q + (W_y + g) \sin q), \\ \lambda &= \left\{ \dot{q}^2 - \frac{1}{\rho} [W_x \sin q - (W_y + g) \cos q] \right\} m. \end{aligned} \quad (2.15)$$

Using λ , we can determine the normal reaction N from (2.7).

The equation of motion of the system in Fig. 1b and the multiplier λ can also be obtained from (2.11) and (2.12) using the constraint equations (1.10) and (1.16) given in terms of functions of the parameter β . Differentiating these equations with respect to β , i.e.,

$$f_1' = x_2' = (R - r)(1 + \cos \beta), \quad f_1'' = -(R - r) \sin \beta, \quad (2.16)$$

$$f_2' = y_2' = (R - r) \sin \beta, \quad f_2'' = (R - r) \cos \beta, \quad (2.17)$$

we arrive at the differential equation of motion and multiplier λ for the determination of N :

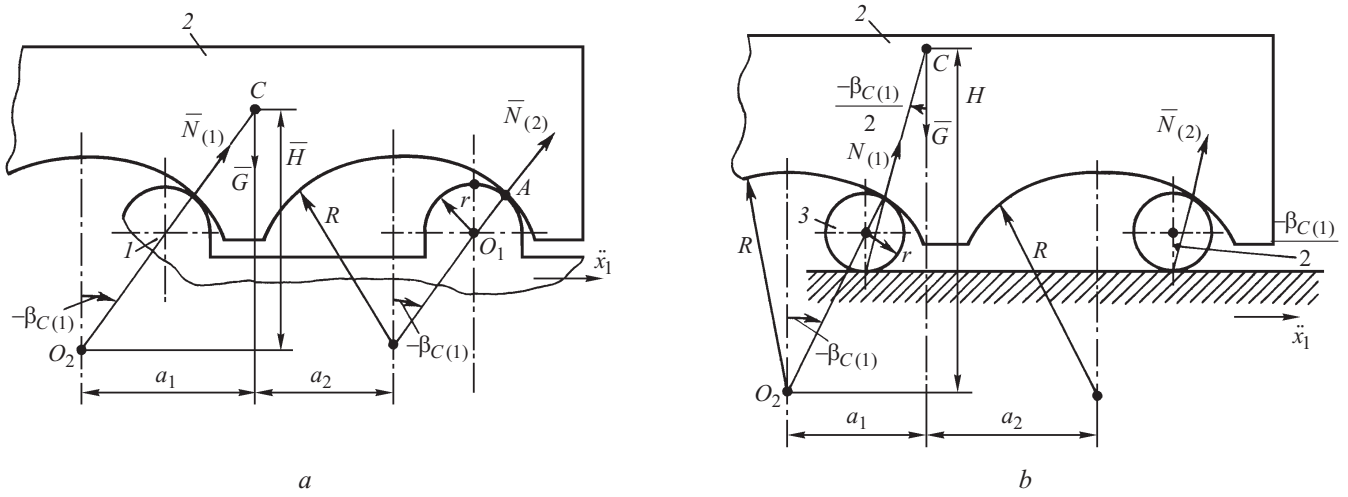


Fig. 2

$$\ddot{\beta} = -\frac{\ddot{x}_1}{2(R-r)} + \frac{\dot{\beta}^2}{2} \tan \frac{\beta}{2} - \frac{g \tan \frac{\beta}{2}}{2(R-r)}, \quad (2.18)$$

$$\lambda = m \left[\frac{\dot{\beta}^2}{2} - \frac{\ddot{x}_1 \tan \frac{\beta}{2}}{2(R-r)} + \frac{g + \ddot{y}_1}{2(R-r)} \right], \quad (2.19)$$

where g is the acceleration of gravity; $\ddot{x}_1 = W_x$ is the acceleration of body 1.

We need to know the reaction N (2.7) to determine the structure (to describe) the system under consideration: it should change as soon as the reaction becomes zero, with a tendency toward negative values. After that, the mechanical system will acquire additional degrees of freedom since constraint reactions will no longer act on it, the unilateral reactions N become zero in this case. Naturally, this case should be completely excluded by choosing such designs and parameters of shock-absorbers that no impacts would occur upon restoration of the system after separation.

3. Applicability Limits of Model (2.11), (2.12). Since each of the reactions N is the sum of two reactions from left “(1)” and right “(2)” supports, i.e.,

$$N = N_{(1)} + N_{(2)}, \quad (3.1)$$

and, moreover, the center of mass C is located above the horizontal line running through the centers O_1 of the surfaces of juts (Fig. 1a) or O_3 for bodies 3 (Fig. 1b), there is a need for an additional analysis to ensure the normal operation of the system during which the reactions $N_{(i)}, i = 1, 2$, of both supports cannot become zero and body 2 is in contact with both supports all the time (there are no impacts). The limiting (critical) angle $\beta_{C(1)}$ at which the reaction of the second support becomes zero corresponds to the configuration in which the vector of the reaction of the first support runs through the center of mass C (Fig. 2).

With further increase in $|\beta_{C(1)}|$, the dynamic equilibrium of the systems could be achieved only if $N_{(2)} < 0$, which is impossible because the geometrical constraints between body 2 and both supports are unilateral. The same is true of support 1. The geometry of the systems in Figs. 1a and 2a suggest that such critical angles are expressed as

$$\beta_{C(1)} = -\arctan \frac{a_1}{H}, \quad \beta_{C(2)} = \arctan \frac{a_2}{H}, \quad (3.2)$$

where a_1 and a_2 are the horizontal distances from the center of mass C of body 2 to the centers O_2 of the spherical surfaces on this body; H is the vertical distance from the point C to the same centers. Thus, the angle β must satisfy the inequality

$$\beta_{C(1)} < \beta < \beta_{C(2)}. \quad (3.3)$$

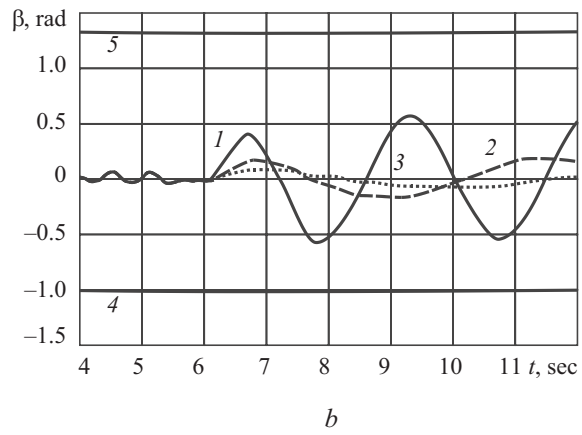
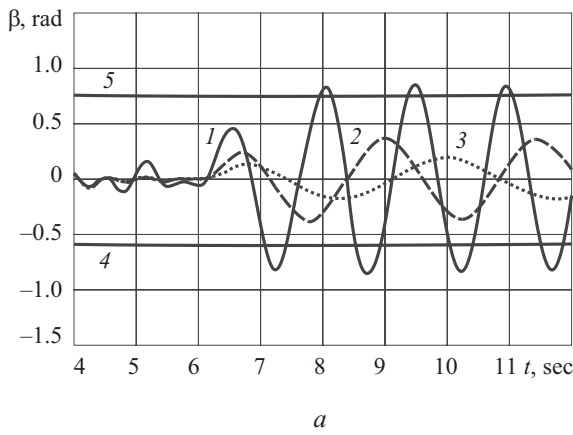


Fig. 3

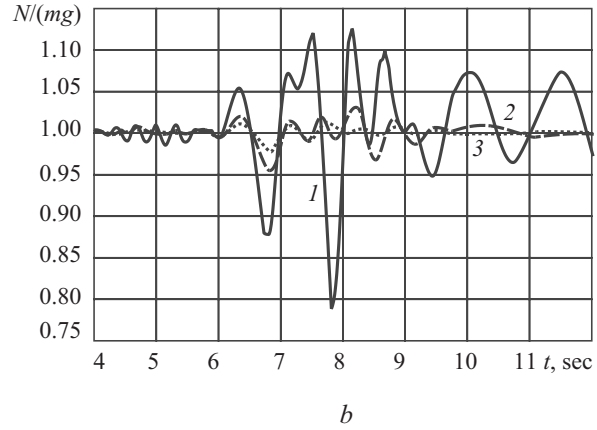
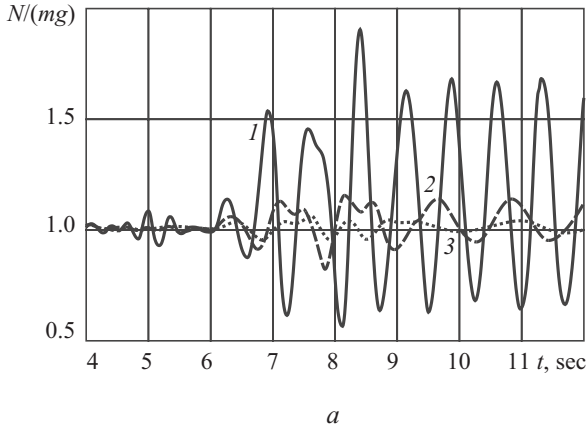


Fig. 4

For the system in Figs. 1b and 2b, the critical angles for the left and right supports are given by

$$\beta_{C(1)} = -2\arctan\left(\frac{a_1}{R+H}\right), \quad \beta_{C(2)} = 2\arctan\left(\frac{a_2}{R+H}\right), \quad (3.4)$$

and the admissible angle β should also be determined from (3.3).

If the contact at the point A (Fig. 1a) and the points A_1 and A_2 (Fig. 1b) is not broken, the coordinates x_2 and y_2 will be defined by (1.1) and (1.2) and by (1.10) and (1.16), respectively.

4. Numerical Example. Since seismic loads are of short duration, it appears reasonable to follow a deterministic approach to study the dynamic processes excited in buildings and other structures. For this purpose, use is often made of input perturbations in the form of sums of products of exponential and harmonic functions.

Figure 3 shows some variables characterizing the behavior of the systems in Fig. 1 and obtained through the numerical integration of the above dynamic systems. The perturbation along the Ox -axis has the following form [8]:

$$\ddot{x}_1 = \sum_{i=1}^7 \left\{ A_i \varepsilon_i \exp\left[-\varepsilon_i^2 (t-t_{O_i})^2\right] \sin\left[\omega_i (t-t_{O_i})\right] \right\}, \quad (4.1)$$

where

$$A_i \text{ [m}\cdot\text{sec}^{-2}\text{]: } 0.28, 1, 4, 2, 3, 0.8, 0.3; \quad \varepsilon_i: 1, 0.5, 1.5, 1, 0.4, 1;$$

$$t_{O_i} \text{ [sec]: } 1, 3, 5, 6.5, 8, 10, 10.5; \quad \omega_i \text{ [sec}^{-1}\text{]: } 6, 8, 10, 4, 9, 7, 6.$$

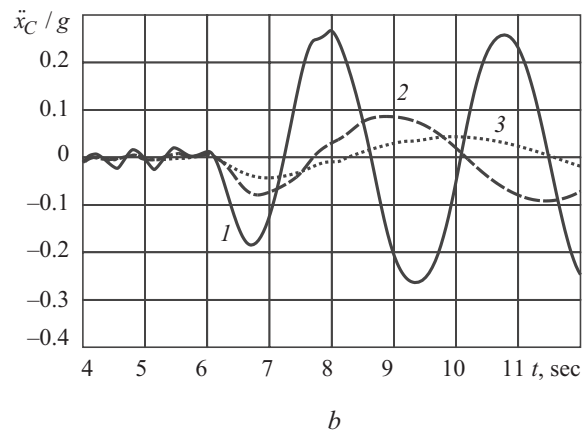
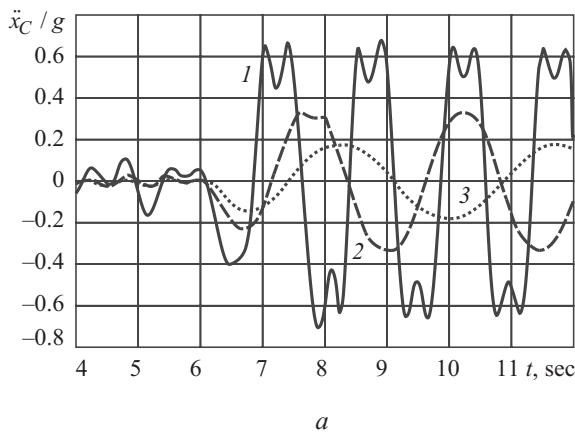


Fig. 5

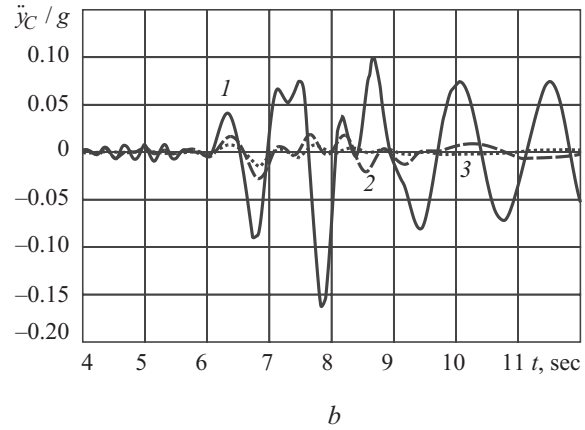
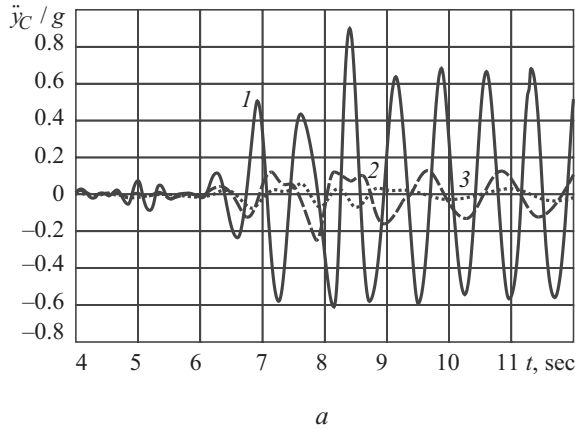


Fig. 6

Moreover, $r=0.1$ m, $a_1 = 10$ m, $a_2 = 14$ m, $H = 15$ m. The vertical vibrations of body 1 are not considered.

Figures 3–6 present the numerical results for the systems in Fig. 1. Curves 1, 2, and 3 correspond to $R-r=0.5, 1.5, 3$ m. Figure 3 shows the variation in the angle β between the vertical and the normal at the contact point of the spherical surfaces. It should be noted that the amplitude of almost steady-state (in β) vibrations in the system with rolling supports (Fig. 1b) is far below that in the system with pure slipping (Fig. 1a), which is true at the frequencies of excited vibrations. Lines 4 and 5 in Fig. 3 represent the critical angles $\beta_{C(1)}$ and $\beta_{C(2)}$ defined by (3.2) and (3.4). It can be seen that when $R-r=0.5$ m (curve 1), the extreme values of the angle β exceed the maximum permissible critical values (3.2) in the system with pure slipping (Fig. 1a), whereas there is a considerable margin for the critical angles (3.4) in the system with supports 3 (Fig. 1b), i.e., the constraints between supports 3 and body 2 are not broken. The pattern for the resultants N (divided by mg) in Fig. 4 is qualitatively similar; they are much smaller in the system in Fig. 1b. Figure 5 shows the projections of the absolute accelerations of bodies 2 (divided by the acceleration of gravity, i.e., \ddot{x}_C / g) onto the Ox -axis and confirm the undeniable advantage of the system with rolling supports 3.

Figure 6 shows the vertical accelerations \ddot{y}_C (divided by g) of body 2, which also demonstrate weaker inertial effects in the system in Fig. 1b.

The above solutions permit the natural conclusion that the system in Fig. 1b is much more preferable to the system in Fig. 1a due to the smaller extreme values of the angle β , vertical displacements of body 2, the projections of its absolute accelerations onto the Ox - and Oy -axes, and the reactions at the contact points between body 2 and the supports (spherical juts or bodies 3). One more important advantage of the system with supports 3 is the higher (in absolute value) critical angles $\beta_{C(i)}$ at which the constraints at the contact points of the spherical surfaces are broken. Moreover, the vertical displacements y_2 are larger in the system in Fig. 1a than in the system in Fig. 1b. Buildings and engineering structures designed as in Fig. 1b would be subject to much weaker effects (inertial forces $-m\ddot{x}_C$ and $-m\ddot{y}_C$ and support reactions N), i.e., would possess higher capacity to

survive earthquakes. Since the vertical components of the absolute acceleration of body 2 occurring during seismic vibrations of structures with shock-absorbers can be reduced with the help of, for example, a prestressed element introduced between body 1 and body 2.

Conclusions. We have outlined a mathematical model describing the vibrations of buildings and engineering structures with general-type passive seismic dampers, rigid bodies, and ideal constraints. Two modifications of systems with passive seismic dampers have been considered assuming constancy of their structure. These systems have been studied numerically. The dynamic processes excited in them have been compared.

REFERENCES

1. S. N. Kozhevnikov, *Foundations of Structural Synthesis of Mechanisms* [in Russian], Naukova Dumka, Kyiv (1979).
2. S. N. Kozuakh, "Kinematic supports in seismic isolation systems of buildings," *Stroit. Arkhitekt., Ser. Seismost. Stroit.*, No. 4, 35–38 (1995).
3. A. I. Lurie, *Analytical Mechanics*, Springer, Berlin–New York (2002).
4. S. V. Polyakov, *Earthquake-Resistant Buildings* [in Russian], Vysshaya Shkola, Moscow (1969).
5. L. N. Reshetov, *Design of Rational Mechanisms* [in Russian], Mashinostroenie, Moscow (1972).
6. I. I. Gol'denblat (ed.), *Seismic Stability of Buildings and Engineering Structures* [in Russian], Stroizdat, Moscow (1972).
7. K. V. Abramov and Yu. V. Mikhlin, "Damping of free elastic vibrations in linear systems," *Int. Appl. Mech.*, **41**, No. 2, 203–209 (2005).
8. E. Ya. Antonyuk and N. P. Plakhtienko, "Dynamic processes in a spheroidal seismic-damping mechanism," *Int. Appl. Mech.*, **41**, No. 1, 90–97 (2005).
9. E. Ya. Antonyuk and N. P. Plakhtienko, "Dynamic modes of one seismic-damping mechanism with frictional bonds," *Int. Appl. Mech.*, **40**, No. 6, 702–708 (2004).
10. A. M. Bloch, M. Reyhanoglu, and N. H. McClamroch, "Control and stabilization of nonholonomic dynamic systems," *IEEE Trans. Automat. Contr.*, **37**, No. 11, 1746–1757 (1992).
11. M. Iiba, M. Midorikawa, H. Yamanouchi, Sh. Yamaguchi, Y. Ohashi, and M. Takayama, "Shaking table tests on performance of isolators for houses subjected to three-dimensional earthquake motions," *I2WCEE*, No. 1765, 1–8 (2000).
12. V. B. Larin, E. Ya. Antonyuk, and V. M. Matiyasevich, "Modeling wheeled machines," *Int. Appl. Mech.*, **34**, No. 1, 93–100 (1998).
13. V. B. Larin and V. M. Matiyasevich, "A control algorithm for a 3D hopping machine," *Int. Appl. Mech.*, **40**, No. 4, 462–470 (2004).
14. A. A. Martynyuk and N. V. Nikitina, "Nonlinear oscillations in a system with dry friction," *Int. Appl. Mech.*, **41**, No. 4, 435–440 (2005).
15. Yu. V. Mikhlin and S. N. Reshetnikova, "Dynamic analysis of a two-mass system with essentially nonlinear vibration damping," *Int. Appl. Mech.*, **41**, No. 1, 77–84 (2005).
16. N. P. Plakhtienko, "Nonlinear translational vibrations of a solid with a gravity–friction seismic damper," *Int. Appl. Mech.*, **39**, No. 9, 1093–1098 (2003).
17. N. P. Plakhtienko, "Nonlinear one-dimensional seismodynamic model of a solid with shock absorbing supports," *Int. Appl. Mech.*, **41**, No. 3, 336–344 (2005).